OPTOELECTRONICS AND ADVANCED MATERIALS – RAPID COMMUNICATIONS Vol. 7, No. 9-10, September - October 2013, p. 692 - 697

New way for synthesis of porous silicon using ion implantation

A. L. STEPANOV[a,b,*], A. A. TRIFONOV[b], Y. N. OSIN[b], V. F. VALEEV[a], V. I. NUZHDIN[a]
[a]*Kazan Physical-Technical Institute, Russian Academy of Sciences, 420029, Kazan, Russia*
[b]*Kazan Federal University, 420008, Kazan, Russia*

A novel idea to create a porous silicon layers by low-energy high-dose metal-ion implantation was realized. To demonstrate a possibility for this technique Ag-ion implantation into monocrystalline silicone substrate was provided. Silicon plates were implanted at energy 30 keV with doses of 7.5×10^{16} - 1.5×10^{17} ion/cm^2 at room temperature. Surface porous structures were analyzed by scanning electron microscope images and energy-dispersive X-ray data. It is shown that the average sizes of porous are increasing approximately from 70 to 120 μm with an increasing of ion doses. The formation of silver nanoparticles inside porous silicon walls was also observed. Novel developed technology based on ion implantation is suggested to give a new way for using of porous layer structures combined with the silicon matrix for various applications.

(Received May 10, 2013; accepted September 18, 2013)

Keywords: Porous silicon, Silver nanoparticles, Ion implantation

1. Introduction

Porous materials have attracted remarkable concerns and found tremendous importance widespread in both fundamental research and industrial applications. Such materials could be widely used for variety applications as absorbents, lightings, catalysts, and for biological molecular filtration and isolation. One quite known method for preparation of porous semiconductor structures is the ion implantation, which was successfully used to create porous germanium layers by Ge^+-, Bi^+- and Sn^+-ion irradiation of crystalline germanium substrates [1-5]. It was also shown that ion implantation could by applied to produce porous structures in amorphous germanium and SiGe (90 % of germanium) alloys thin films [6]. Ion implantation is a well established and all over the world accessible technique, which being mainly used for semiconductor microelectronic device fabrication. The pore size and the pore depth could be controlled and tuned by the ion implantation parameters such as the ion dose and energy. Unfortunately, a question about a possibility to synthesize the porous silicon (PSi) using such technological way by present time was open.

At present PSi is considering as a key material in many industrial sectors as electronics, sensors and photonics. PSi was first obtained in the mid-1950s at Bell Labs [7], but it was not seriously used until the discovery of its strong luminescent properties in 1990 [8]. Prior to this discovery, PSi was almost exclusively considered as insulating layer devices in the microelectronics industry [9]. However, in the last decade the great potential of PSi in a wide range of fields was demonstrated, from opto- and microelectronics to biomedicine, biological, medicine and chemical sensing, optics, etc. [9, 10]. In past there were only two main technological methods for production of PSi structures: electrochemical etching and chemical stain etching. Thus, PSi could be chemically created on silicon under the appropriate conditions with typical feature porous sizes in the order of a few nanometers [9, 11]. Both the porosity and the pore morphology of PSi are greatly influenced by the electrochemical and chemical stain etching parameters. As it was mentioned here the ion implantation technique for fabrication of PSi was no used before [6].

Additionally, the interest to Si nanostructures containing noble metal nanoparticles was recently found. It was initiated because metal nanoparticles with localized surface plasmon modes are a specific option to enhance the recombination rate of the light Si emitter to increase the efficiency of photoluminescence and internal quantum effectively [11, 12]. Silver nanoparticles (AgNPs) are the subject of specific increasing interests due to their strongest plasmon resonance in the visible spectrum [13, 14]. For example, PSi samples coated with a layer of AgNPs after their electrochemical etching demonstrated that a photoluminescence intensity becomes remarkably increased [15] or the reflection of incident light with wavelength below 1100 nm could be reduced to use them for antireflection application [16].

Instead of using silicon as the substrate for the AgNPs deposition on the top of a sample, the ion implantation technique can be used to form AgNPs in a volume of silicon as in the case of ion-irradiated silica glass or polymers [14, 17]. In experiments of works [18, 19] Ag-ion implantation into crystalline silicon wafers and silicon nanocrystal layers at energy of 30-35 keV and rather lower dose of 5.0×10^{15} ion/cm^2 was performed. Then AgNPs in silicon matrix were synthesized after thermal annealing at 500°C of implanted samples. In another work [20] a high-dose (2.0×10^{17} ion/cm^2) Ag^+-ion implantation of silicon

using MEVVA source, which produced a mixture of Ag^{n+} ions, was applied to create AgNPs. However, it has to be mentioned that PSi structures in these publications has never been observed after ion implantation [21].

At the present work a novel technological way based on low energy single-ion implantation was suggested and realized to create PSi layers on the crystalline surface of Si wafers. At present work it is demonstrated that using high-dose (more than 1.0×10^{16} ion/cm^2) Ag-ion implantation of silicon with the energy of 30 keV various PSi structures with AgNPs can be successfully fabricated.

2. Experimental

An *p*-type (100)-oriented single crystalline silicon wafers as the substrate were used for Ag-ion implantation to create PSi structures. The substrates were cleaned in a wet chemical etching process. The silicon wafers were implanted with Ag^+ ions at 30 keV with doses in the range between 7.5×10^{16} and 1.5×10^{17} ion/cm^2 and at ion current density of 4 μA/cm^2 using the ion beam implanted ILU-3 at residual vacuum of 10^{-5} Torr and at room temperature of the irradiated samples.

Some silicon substrates were implanted through a mask consisting of a mesh nickel grid with square holes and bar width of 40 μm. In this way, selectively implanted regions next to unimplanted ones were prepared in order to perform the step-height analysis.

Depth distribution profiles of Ag atoms and the damage level in implanted silicon were modeled using the simulation-program the Stopping and Range of Ions in Matter (SRIM-2012) [22]. The morphology of the implanted samples were characterized in plan-view by scanning electron microscopy (SEM) using microscope Merlin Zeiss combined with ASB (Angle Selective Backscattering) and ESB InLens (Energy selective Backscattering) detectors and equipped for energy-dispersive X-ray spectroscopy (EDX) analysis with device AZtec X-MAX from Oxford Instruments with resolution of 127 eV. Focusing ion beam (FIB) technique was applied to provide a milling of implanted silicon surface for analyzing a sample depth by Auriga CrossBeam Workstation Ziess (FIB-SEM) with 30 KeV Ga liquid metal ion source at normal incidence. By this approach square of 2 × 2 μm on a PSi surface was written at ion current density of 50 nA that did not heat a sample but sputtere a surface.

3. Results and discussion

According to the SRIM simulations, during ion bombardment an excess vacancy-rich region can be formed close to the surface and excess implanted ions are ranged deeper in irradiated matrix (Fig. 1). A mean penetration range (R_p^{Ag}) of 30 keV accelerated Ag^+-ions into silicon substrate is about with 26 nm with a longitudinal straggling (ΔR_p^{Ag}) of 8 nm in the Gaussian depth distribution (Fig. 1a). Thus the assumed thickness of the modified silicon surface layer ($R_p + 2\Delta R_p$) is about 42 nm. Since it was assumed [23] that porous semiconductor structure, for example, in germanium results from nucleation of small voids in the amorphous state by vacancy accumulations during ion implantation, the vacancy depth distribution in silicon implanted with Ag^+ ions was also simulated by the SRIM (Fig. 1b). Annualizing SRIM modeling, however it should be taking in account that obtained depth distribution of Ag ions and vacancies are corresponded to implantation process into uniform silicon matrix before a nucleation and growth (for ion dose less then 1.0×10^{16} ion/cm^2) of PSi and therefore, only qualitative estimation of such distributions in silicon should be considered.

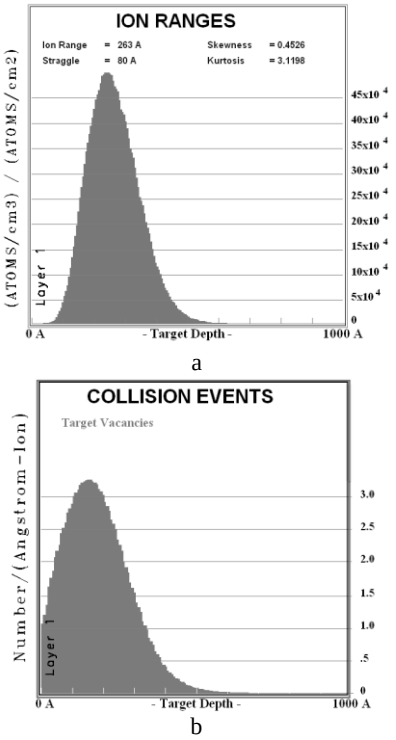

Fig. 1. Depth ion distribution of Ag-ions implanted (a) and generated vacancy profiles (b) in silicon with energy of 30 keV calculated using the SRIM Ag code.

Fig. 2 shows a plane-view SEM image of unimplanted silicon, which looks likes as very smooth without any surface structural inhomogeneity. The results of porosification of the silicon samples observed by plan-view SEM (Fig. 3 a, b, c). In contrast to unimplanted silicon (Fig. 2) the characteristic PSi surface structure causes the black hole appearance in the implanted silicon region. They are consisting of cellular features partitioned by rather thin walls which are clearly resolved in all samples which were formed by various Ag-ion dose irradiation: 7.5×10^{16}, 1.0×10^{17} and 1.5×10^{17} ion/cm^2. Uniform pore distributions with distinguished sharp holes over all implanted surfaces on silicon-implanted samples were observed. The size values of pores was measured by counting the number of holes in several micrographs, taking into account all visible holes boundaries and subtracting those holes that intersects an edge of the SEM image. From this, the size of the pores was estimated. It is seen that mean size of pores (black holes) increasing in

magnitude with an increasing of Ag-ion doses with estimated average range 70 to 120 μm, respectively. The SEM images with different scales corresponding to the sample implanted at highest dose of 1.5×10^{17} ion/cm^2 presented in Fig. 4. A white spots in these figures corresponds to material with higher density against to silicon that suggests them to be AgNPs.

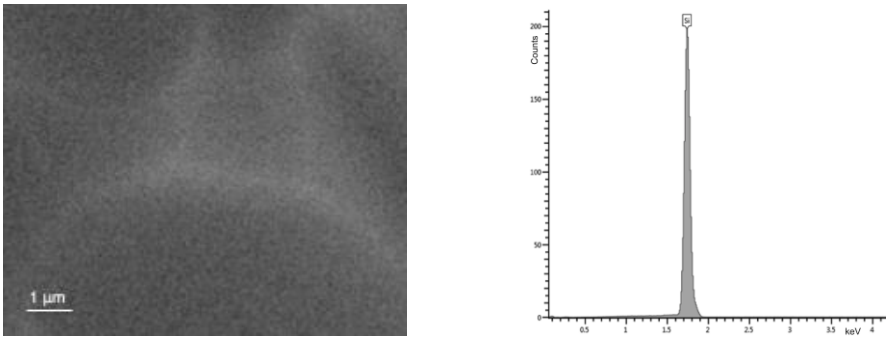

a b

Fig. 2. SEM image (a) and EDX characteristic spectrum (b) of unimplanted silicon surface.

In Fig. 2b and 3(c, e, f) it is shown a standard EDX spectra recorded on the examined silicon and PSi with AgNPs samples, respectively. EDX measurements for implanted samples were done in the area on surface sample outside black holes of the silicon pores. In contrast to unimplanted silicon (Fig. 2b), in the middle part of the presented spectra of PSi it is clear seen four peaks located between 2.5 and 3.5 keV. Those maxima are directly related to the Ag characteristic lines. Thus the spectra obtained during EDX studies could be used for carrying out the quantitate analysis of Au contends. The intensity of Ag EDX peaks was increased for higher ion implantation dose that demonstrates increasing of Ag concentrations in the silicon samples. Appearance of Ag peaks is in consistence with white sports in SEM images of the PSi, which are corresponding to AgNPs synthesized in PSi during ion implantation (Fig. 4). As shown in present study, using selected conditions for low-energy Ag-ion irradiation of silicon AgNPs can be fabricated without post-implantation thermal annealing as it was applied in the works [11, 12].

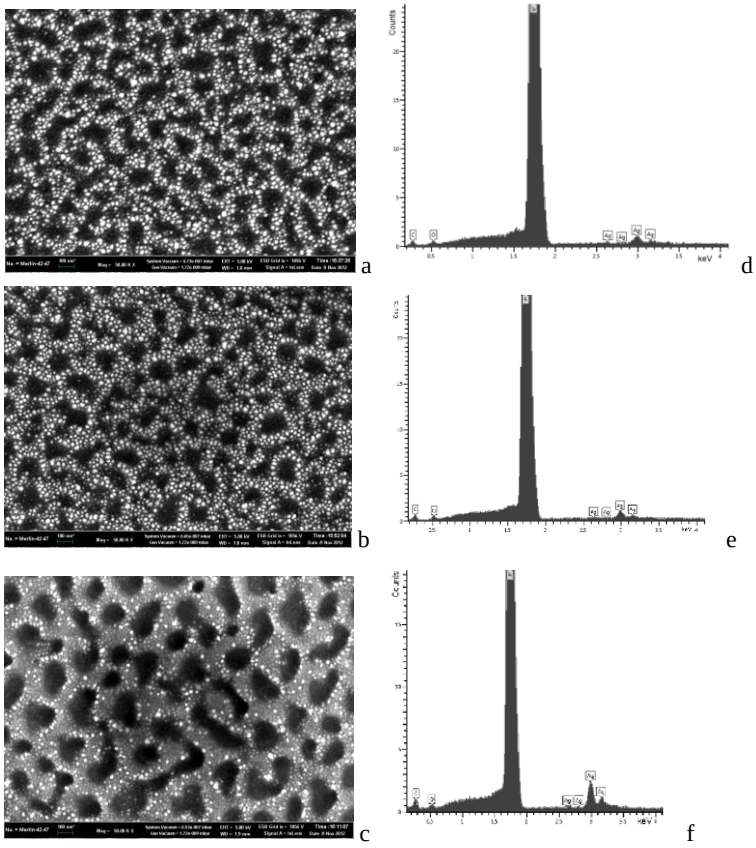

a d b e c f

Fig. 3. SEM images and EDX characteristic spectrum of PSi fabricated at various doses: (a) 7.5 $\times 10^{16}$; (b) 1.0 $\times 10^{17}$ and 1.5 $\times 10^{17}$ ion/cm^2. Visible EDX peaks confirm the presence of Ag in the synthesized PSi strictures.

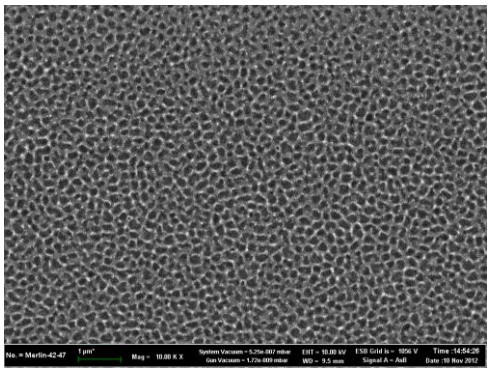

a

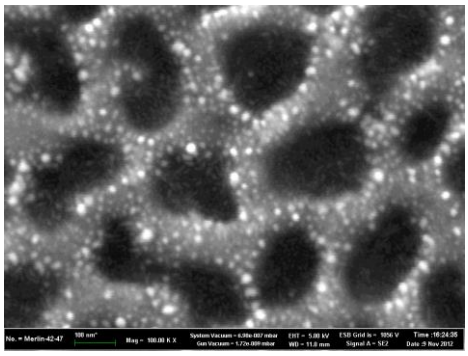

b

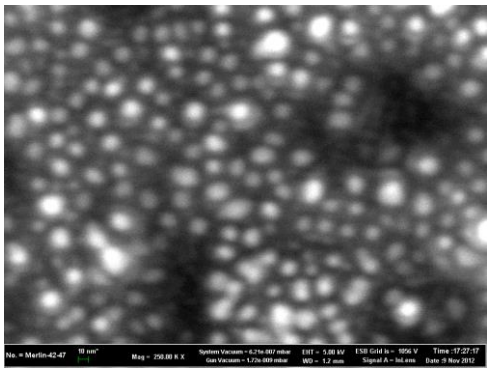

c

Fig. 4. SEM images of PSi structure fabricated at a dose of 1.5×10^{17} ion/cm^2 presented with different scales.

For the applied FIB conditions of PSi treatment, the mean penetration depth of Ga^+-ions implanted into silicon was obtained by SRIM calculation, which gives a value R_p^{Ga} = 28 nm with a straggling (ΔR_p^{Ga}) of 10 nm in the Gaussian depth distribution. Fig. 5 represents a SEM image of a FIB-milled cross-section of a 30 keV, 1.5×10^{17} ion/cm^2 irradiated area of the surface with PSi. The whole thickness of the affected layer is about 1 μm. On the walls of a recess a more or less closed short columnar structure (shown by arrows) with approximately size of several tens nanometers could be recognized, which is expends from the surface to the depth of the sample.

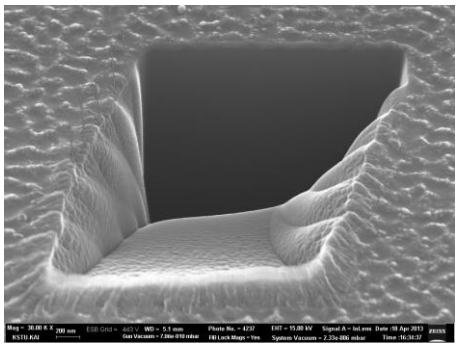

Fig. 5. SEM image of sample surface with PSi structures (as in Fig. 4) fabricated at an Ag^+-ion dose of 1.5×10^{17} ion/cm^2 after FIB treatment with Ga ions. Gray arrows show top positions of vertically continued porous on the wall of a recess in the FIB-milled cross-section.

The Fig. 6a shows the step-height measured for silicon implanted with a dose of 1.5×10^{17} ion/cm^2 and which was carried out on the sample selectively implanted through the nickel grid (Fig. 6d). The picture of nickel grid was collected with optical microscope Axio Image 2 Zeiss. The image of unimplanted silicon region corresponds to dark area whereas implanted PSi structures are presented as a light gray squares (Figs. 6a and 6b). The spattering of the implanted with respect of the unimplanted region is determined as illustrated in the insert of Fig. 6c. In first approximation, it can be speculated that the volume expansion is related to a mechanism simply governed by the nuclear energy deposition, which is usually measured in displacement per atom.

It is known that for a critical rather-low implantation dose, silicon undergoes a crystalline to amorphous phase transition [24, 25]. As seen in present experiments at higher doses exhibit voiding within the amorphous silicon layer forms a porous structure with AgNP inclusions. Thus, as the first time in practice, it is demonstrated by present experiment that PSi growth was stimulated by high-dose metal-ion implantation. This new result for silicon could be considered in consistence with published data about porous germanium fabrication during ion implantation process [1, 6, 26, 27] and suited possible mechanism for PSi structuring could be assumed.

Despite PSi creation by metal-ion implantation of silicon, in case of germanium over the past 30 years there was much debate as to what mechanism governs the formation of the porous semiconductor structure in ion implanted germanium [5]. Currently, there are two main theories of void formation for germanium: vacancy clustering and so-called **"**microexplosions**"**. The vacancy clustering theory invokes the inefficient recombination of germanium point defects during ion-implantation, where once a critical point defect population is created by ion-implantation, excess vacancies cluster into pores in order to minimize the dangling bond density. In contrast, the microexplosion theory is based on the creation of voids through pressure waves and thermal spikes caused by the overlap of ion cascades [5]. Therefore, in principle, it is

possible to determine which theory better models void and porous formation in silicon by selecting appropriate implant conditions and observing the resulting microstructure after implantation. Thus, additional experimental study of PSi fabrication by high-dose ion implantation of silicon is necessary and such work will be continued.

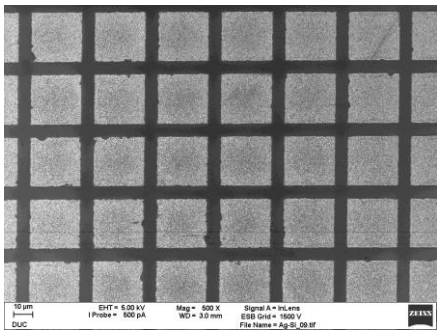

a

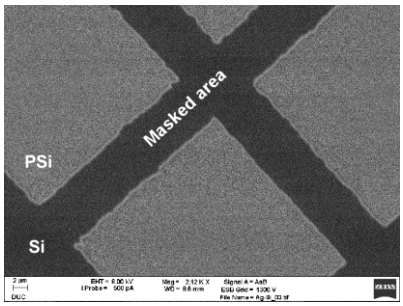

b

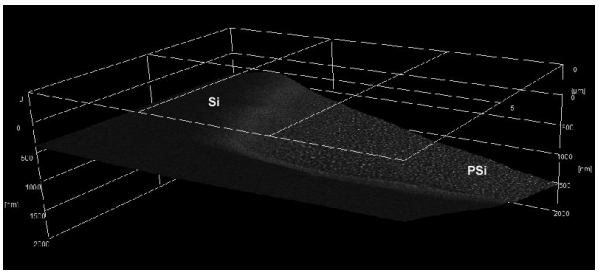

c

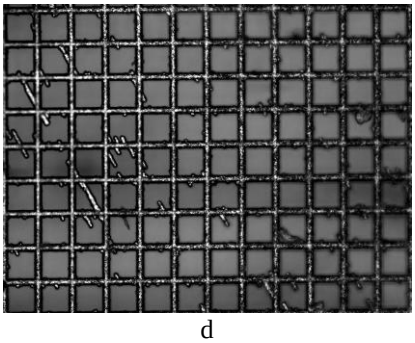

d

Fig. 6. (a) and (b) SEM image (different scales) of structures with PSi (light gray) fabricated at a Ag^+-ion dose of 1.5 ×10^{17} ion/cm^2 through a mesh nickel mask used to analyze the step-height between unimplanted silicon (dark gray) covered during irradiation with the mask and implanted regions with PSi (light area), (c) 3D SEM reconstruction of step area which demonstrates a sputtering of the silicon surface during Ag-ion implantation and (d) optical microscope image of the nickel grid.

4. Conclusion

In conclusion, the first result on a novel technique for PSi structuring on silicon wafers combined with AgNPs, which are nucleation and growth inside PSi walls, using low energy high dose ion implantation was presented. Formation of porous material with AgNPs for various ion doses was directly evident by SEM and EDX analysis. The new developed nanostructuring porous semiconductor material with metal nanopartilces is a subject for following study of optical plasmonic, photoluminescence, antireflection, nonlinear-optical and biosensor perspective properties.

Acknowledgements

A.L.S. grateful to the Alexander von Humboldt Foundation and the DAAD (Germany). Also, this work was partly supported by the Russian Foundation for Basic Research (Nos. 11-02-91341, 11-02-90420, 12-02-97029, 12-02-00528 and 13-02-12012) and NIR KFU 13-56.

References

[1] I. H. Wilson, J. Appl. Phys. **53**, 1698 (1982).
[2] B. R. Appleton, O. W. Holland, D. B. Poker, J. Narayan, D. Fathy, Nucl. Instr. Meth. Phys. Res. B **7-8**, 639 (1985).
[3] O. W. Holland, B. R. Appleton, J. Narayan, D. Fathy, J. Appl. Phys. **54**, 2295 (1985).
[4] G. G. Zakirov, G. D. Ivlev, I. B. Khaibullin, Sov. Phys. Semicond. USSA **22**, 598 (1988).
[5] B. L. Darby, B. R. Yates, N. G. Rudawski, K. S. Jones, A. Kontos, R. G. Elliman, Thin Solid Films **519**, 5962 (2011).
[6] L. Romano, G. Impellizzeri, L. Bosco, F. Ruffino, M. Miritello, G. Grimaldi, J. Appl. Phys. **111**, 113515 (2012).
[7] A. Uglir, Bell Syst. Tech. J. **35**, 333 (1956).
[8] L. T. Canham, Appl. Phys. Lett. **57**, 1046 (1990).
[9] V. Torres-Costa, R. J. Martin-Palma, J. Mater. Sci. **45**, 2823 (2010).
[10] V. S.-L. Lin, K. Motesharei, K. P.-S. Dancil, M. J. Sailor, M.R. Ghadiri, Science **278**, 840 (1997).
[11] G. Oskam, J. G. Long, A. Natarajan, P. C. Searson, J. Phys. D: Appl. Phys. **31**, 1927 (1998).
[12] T. S. Amran, M. R. Hashim, N. K. Al-Obaidi, H. Yazid, R. Adnan, Nanoscale Research Lett. **8**, 35 (2013).
[13] U. Kreibig, M. Vollmer, Optical properties of metal clusters, Springer, Berlin, 1995.
[14] A. L. Stepanov, Ion-synthesis of silver nanoparticles \ and their optical properties. Nova Sci. Publ., New York, 2010.
[15] D. T. Cao, L. T. Q. Ngan, C. T. Anh, Surf. Interface Anal. **45**, 762 (2013).
[16] Y. Wang, Y. P. Liu, H. L. Liang, Z. X. Mei, X. L. Du, Phys. Chem. Chem. Phys. **15**, 2345 (2013).

[17] A. L. Stepanov, Tech. Phys. **49**, 143 (2004).
[18] A. K. Sing, K. G. Gryczynski, F. D. McDaniel, S. Y. Park, M. Kim, A. Neogi, Appl. Phys. Express **3**, 102201 (2010).
[19] A. K. Sing, K. G. Gryczynski, A. Neogi, Opt. Mater. Express **2**, 501 (2012).
[20] H. W. Seo, Q. Y. Chen, I. A. Rusakova, Z. H. Zhang, D. Wijesundera, S. W. Yeh, X. M. Wang, L. W. Tu, N. J. Ho, Y. G. Wu, H. X. Zhang, W. K. Chu, Nucl. Instr. Meth. Phys. Res. B **292**, 50 (2012).
[21] L. Romano, G. Impellizzeri, M. V. Tomasello, F. Giannazzo, C. Spinella, M. G. Grimaldi, J. Appl. Phys. **107**, 84310 (2010).
[22] J. F. Ziegler, J. P. Biersack, U. Littmark, The Stopping and Range of Ions in Solids, Pergamon Press, New York, 1985.
[23] L. M. Wang, R. C. Birtcher, Appl. Phys. Lett. **55**, 2494 (1989).
[24] E. Chason, S. T. Picraux, J. M. Poate, J. O. Borland, M. I. Current, T. Diaz de la Rubia, D. J. Eaglesham, O. W. Holland, M. E. Law, C. W. Mayer, J. Melngails, A. F. Tasch, J. Appl. Phys. **81**, 6513 (1997).
[25] J. S. Williams, Mater. Sci. Eng. A **253**, 8 (1998).
[26] T. M. Donovan, K. Heinemann, Phys. Rev. Lett. **27**, 1794 (1971).
[27] T. Steinbach, J. Wemecke, P. Kluth, M. C. Ridgway, W. Wesch, Phys. Rev. B **35**, 104108 (1987).

* Corresponding author: aanstep@gmail.com